Available online at www.sciencedirect.com

ScienceDirect

Advances in Space Research xxx (2017) xxx–xxx

ADVANCES IN SPACE RESEARCH (a COSPAR publication)

www.elsevier.com/locate/asr

# Coastal sea level from CryoSat-2 SARIn altimetry in Norway

Martina Idžanović [a,*], Vegard Ophaug [a], Ole Baltazar Andersen [b]

[a] Faculty of Science and Technology, Norwegian University of Life Sciences (NMBU), Drøbakveien 31, N-1430 Ås, Norway
[b] DTU Space, Technical University of Denmark, Elektrovej, DK-2800 Kgs. Lyngby, Denmark

Received 16 August 2016; received in revised form 26 July 2017; accepted 30 July 2017

**Abstract**

Conventional (pulse-limited) altimeters determine the sea surface height with an accuracy of a few centimeters over the open ocean. Sea surface heights and tide-gauge sea level serve as each other's buddy check. However, in coastal areas, altimetry suffers from numerous effects, which degrade its quality. The Norwegian coast adds further challenges due to its complex coastline with many islands, mountains, and deep, narrow fjords.

The European Space Agency CryoSat-2 satellite carries a synthetic aperture interferometric radar altimeter, which is able to observe sea level closer to the coast than conventional altimeters. In this study, we explore the potential of CryoSat-2 to provide valid observations in the Norwegian coastal zone. We do this by comparing time series of CryoSat-2 sea level anomalies with time series of in situ sea level at 22 tide gauges, where the CryoSat-2 sea level anomalies are averaged in a 45-km area around each tide gauge. For all tide gauges, CryoSat-2 shows standard deviations of differences and correlations of 16 cm and 61%, respectively. We further identify the ocean tide and inverted barometer geophysical corrections as the most crucial, and note that a large amount of observations at land-confined tide gauges are not assigned an ocean tide value. With the availability of local air pressure observations and ocean tide predictions, we substitute the standard inverted barometric and ocean tide corrections with local corrections. This gives an improvement of 24% (to 12.2 cm) and 12% (to 68%) in terms of standard deviations of differences and correlations, respectively.

Finally, we perform the same in situ analysis using data from three conventional altimetry missions, Envisat, SARAL/AltiKa, and Jason-2. For all tide gauges, the conventional altimetry missions show an average agreement of 11 cm and 60% in terms of standard deviations of differences and correlations, respectively. There is a tendency that results improve with decreasing distance to the tide gauge and a smaller footprint, underlining the potential of SAR altimetry in coastal zones.


*Keywords:* CryoSat-2; SARIn altimetry; Tide gauges

## 1. Introduction

Satellite altimetry is a well-proven and mature technique for observing the sea surface height (SSH) with an accuracy of a few centimeters over the open ocean (Chelton et al., 2001). The effective footprint of an altimeter is controlled by the pulse duration and width of the analysis window, and is typically between 2 and 7 km, depending on the sea state (Gommenginger et al., 2011). These classic pulse-limited altimeter systems are often termed conventional altimeters (Vignudelli et al., 2011). For such altimeters and typical wave heights of 3–5 m, a circular footprint of ~100 km$^2$ is obtained, depending on the satellite orbit (Chelton et al., 1989).

The coastal zone is particularly relevant to society considering, e.g., sea-level rise, shipping, fishery, and other offshore activities (Pugh and Woodworth, 2014). The application of satellite altimetry is difficult close to the coast due to land and calm-water (bright target) contami-

* Corresponding author.
*E-mail address:* maid@nmbu.no (M. Idžanović).

http://dx.doi.org/10.1016/j.asr.2017.07.043
0273-1177/

nation of the radar echoes. This, in combination with a degradation of key range (wet troposphere) and geophysical corrections (high-frequency atmospheric and ocean signals, and tides), results in observation gaps in these zones (Vignudelli et al., 2005, 2011; Saraceno et al., 2008; Gómez-Enri et al., 2010). Large variations in atmospheric pressure along the coast and complex tidal patterns degrade the geophysical corrections for dynamic atmosphere and ocean tides (Andersen and Scharroo, 2011). Considering that Norway has the world's second longest coastline of 103,000 km, with many islands, steep mountains, and deep narrow fjords, the application of coastal altimetry is especially challenging there. An impression of the conventional altimetry observation gap along the Norwegian coast is given in a recent comparison of conventional altimetry with tide gauges (TGs). The average distance between valid points of crossing conventional altimetry tracks and local TGs was ~54 km (Ophaug et al., 2015).

The European Space Agency (ESA) CryoSat-2 (CS2) is the first new-generation altimetry satellite carrying a synthetic aperture interferometric radar altimeter (SIRAL) (Wingham et al., 2006). CS2 can operate in synthetic aperture radar (SAR), interferometric SAR (SARIn), as well as conventional low resolution (LR) modes. At high latitudes, the satellite operates in all three modes following geographically delimited masks. Along the Norwegian coast, in a narrow strip with a typical width of less than ~40 km, CS2 operates in SARIn mode (Fig. 1a). A Delay-Doppler modulation of the altimeter signal creates a synthetic footprint in this mode. The footprint is nominally 0.3 km by 8 km in respectively along- and across-track directions (Table 1). Hence, the risk that the footprint is contaminated by land is far less for CS2 in this mode compared to conventional altimeters.

The main goal of this study is to evaluate CS2 along the Norwegian coast, which comprises degraded SARIn data (without phase information, see Section 2.1). We explore the potential for these data to provide valid sea-level observations closer to the coast than conventional pulse-limited altimetry by comparing time series of CS2 observations with observations from an array of TGs along the Norwegian coast. The same tide-gauge (TG) comparison is also done using three conventional altimetry missions to quantify the performance of CS2 with respect to conventional altimetry. The data and methods are introduced in Section 2, comparison results are shown and discussed in Section 3, and conclusions are presented in Section 4.

## 2. Data and methods

### 2.1. CryoSat-2 20 Hz SARIn data processing

Satellite altimetry is normally distributed through initiatives like AVISO (http://www.aviso.altimetry.fr), OpenADB (http://openadb.dgfi.badw.de), PODAAC (http://podaac.jpl.nasa.gov), and RADS (http://rads.tudelft.nl), focusing on the regular distribution of homogenized and quality-controlled 1 Hz data. However, these archives do not process and/or distribute the CS2 SARIn data. ESA provides CS2 data in two levels, Level 1 (L1) and Level 2 (L2). L1 data contain orbit information and waveforms, while L2 data contain range and geophysical corrections, as well as height estimates. The 20 Hz L1b SARIn dataset was retracked using the simple threshold retracker (Nielsen et al., 2015), whereby the bin that contains 80% of the maximum power is taken as the retracking point. The SARIn dataset was obtained by the Technical University of Denmark (DTU) Space retracker system (Stenseng and Andersen, 2012) for the period from 2010 to 2014, which, at the time of this study, was based on the ice baseline B processor. Since then, it has been replaced by the CS2 baseline C processor (Bouffard et al., 2015). According to Webb and Hall (2016), the altimeter range $R$ is given by

$$R = R_{wd} + R_{retrack} + R_{corr}, \quad (1)$$

where $R_{wd}$ is the window delay, $R_{retrack}$ is the correction obtained in the retracking. $R_{corr}$ are range and geophysical corrections including wet and dry troposphere, ionosphere, and atmospheric and tidal oceanic variations. In turn, the SSH is given by

$$SSH = h - R, \quad (2)$$

where $h$ is the altitude of the satellite. 20 Hz sea level anomalies (SLAs) were computed referencing the sea surface heights (SSHs) to the DTU15 Mean Sea Surface (MSS) (Andersen et al., 2015) and applying range and geophysical corrections (see Section 2.4 and Table 3).

At the time of data processing, the SARIn/cross-track correction (Armitage and Davidson, 2014; Abulaitijiang et al., 2015) was not implemented in the retracker system. Consequently, the SARIn observations are degraded SARIn observations excluding phase information. Because the burst mode pulse repetition frequency in SAR mode is four times that of SARIn mode, the SARIn data are expected only to have half the precision of normal SAR altimetry (Wingham et al., 2006). As this study is a first validation of CS2 along the Norwegian coast, with the most important goal being to explore the potential of SAR altimetry missions (such as Sentinel-3 and Jason-CS/Sentinel-6), we still believe that a study of degraded SARIn CS2 observations is of value.

A suite of editing and outlier detection criteria are normally used to edit the altimeter data for the computation of 1 Hz data, see, e.g., Scharroo et al. (2013). As most of these are not available for the CS2 L1 data, we employed a two-step outlier detection. After discarding all CS2 observations over land using a high-resolution coastline (1:50,000 map scale, provided by the Norwegian Mapping Authority (NMA)) as a mask, the first step in the outlier detection was to remove all observations deviating more than ±1 m from DTU15 MSS. This first step led to a 28% data rejection. The second step of our outlier detection was based on a within-track gross error search using a multiple $t$ test

Please cite this article in press as: Idžanović, M., et al. Coastal sea level from CryoSat-2 SARIn altimetry in Norway. Adv. Space Res. (2017), http://dx.doi.org/10.1016/j.asr.2017.07.043

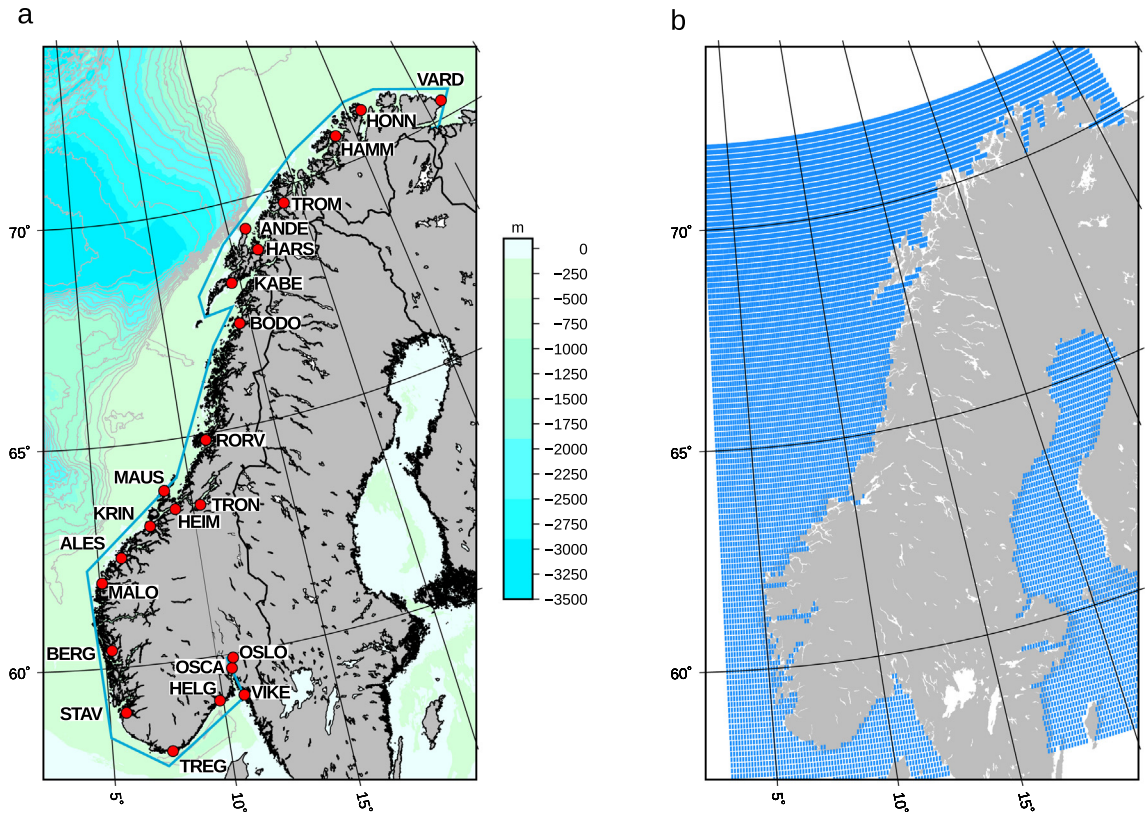


Fig. 1. (a) The 22 Norwegian TGs considered in this study. The blue line shows the CS2 SARIn mode border, using the geographical mode mask version 3.8 (European Space Agency, 2016). Bathymetry and 400 m isobaths are from the 2014 General Bathymetric Charts of the Oceans (GEBCO) (Weatherall et al., 2015). (b) FES2004 grid cells around Norway.

Table 1
CryoSat-2 mission specifications (Webb and Hall, 2016).

| CryoSat-2 | |
|---|---|
| Mission duration | 8 April 2010 – present |
| Frequency | 13.57 GHz |
| Latitudinal limit | 88° |
| Orbit type | Near circular, polar, Low Earth Orbit |
| Altitude | 717 km |
| Inclination | 92° |
| Repeat period | 396 (30) days |
| Footprint size along-track | 2–10 km (250–400 m for SAR) |
| Footprint size across-track | 7.7 km |
| Footprint area | 185.1 km$^2$ (4.9 km$^2$ for SAR) |

(Koch, 1999; Revhaug, 2007), applied to the SLAs. Thus, we allow our SLAs $\mathbf{l}$ $(n \times 1)$ to contain gross errors $\nabla$ $(q \times 1)$, and see that the observation vector can be corrected for those gross errors by the subtraction $\mathbf{l} - \mathbf{E} \cdot \nabla$. Consequently, we extend the linear model by introducing a gross-error term:

$$\mathbf{l} - \mathbf{E} \cdot \nabla + \tilde{\mathbf{v}} = \mathbf{A} \cdot \tilde{\mathbf{x}}, \tag{3}$$

where $\mathbf{E}$ is an $(n \times q)$ matrix containing ones where a gross error is present (at $(n, q)$) and zeros elsewhere. $\mathbf{A}$ is the well-known $(n \times e)$ design matrix. Correcting for gross errors, we obtain new estimates for the residuals $\mathbf{v}$ $(n \times 1)$ and unknowns $\mathbf{x}$ $(e \times 1)$, annotated as $\tilde{\mathbf{v}}$ and $\tilde{\mathbf{x}}$.

A statistical outlier test based on Eq. (3) is obtained if the null hypothesis $H_0 : \nabla = 0$ (all outliers equal zero) is tested against the alternative hypothesis $H_1 : \nabla = \nabla_1 \neq 0$. The least-squares solution for Eq. (3) gives:

$$\mathbf{Q}_\nabla = (\mathbf{E}^T \cdot \mathbf{P} \cdot \mathbf{Q}_v \cdot \mathbf{P} \cdot \mathbf{E})^{-1}, \tag{4}$$

$$\nabla = -\mathbf{Q}_\nabla \cdot \mathbf{E}^T \cdot \mathbf{P} \cdot \mathbf{v}, \tag{5}$$

where $\mathbf{Q}_v$ and $\mathbf{Q}_\nabla$ are cofactor matrices of $\mathbf{v}$ and $\nabla$, respectively, and $\mathbf{P}$ the weight matrix. Applying the multiple $t$ test, one observation at a time can be tested, with an estimated standard deviation of $\nabla$:

$$\tilde{s}^2_\nabla = \frac{1}{f-1} \cdot \left( \mathbf{v}^T \cdot \mathbf{P} \cdot \mathbf{v} - \frac{\nabla^2}{\mathbf{Q}_\nabla} \right), \tag{6}$$

where $f$ represents the degrees of freedom.

First, we assume a solution without gross errors, after which we perform the outlier test. Without the presence of gross errors, $\nabla$ is small and the observations are normally distributed, i.e., $\mu = \mathrm{E}\{\nabla\} = 0$. Then, the $t$-statistic can be written as:

$$t = \frac{\nabla}{s_\nabla}, \tag{7}$$

Please cite this article in press as: Idžanović, M., et al. Coastal sea level from CryoSat-2 SARIn altimetry in Norway. Adv. Space Res. (2017), http://dx.doi.org/10.1016/j.asr.2017.07.043

where $s_\nabla$ is the estimated standard deviation of the gross error. If there is no gross error present, $t$ in Eq. (7) will follow the $t$ distribution. Thus, if the absolute value of $t$ is smaller than the threshold value (two-tailed, with $\alpha = 0.05$ and $f = n - 1$), we accept the observation, otherwise we classify it as an outlier. For further details, see Koch (1999). On average, ~21% of the data points were classified as outliers (Table 2).

### 2.2. Tide-gauge data

We have considered 22 out of 23 TGs on the Norwegian mainland as shown in Fig. 1a, leaving out the Narvik TG due to few CS2 observations. The TG data were provided by NMA (K. Breili, personal communication) with a 10-min sampling rate, and include predicted ocean tides as well as local air pressure observations.

Both inverse barometer (IB) and ocean tide (OT) corrections were applied to the TG observations, making them comparable with the altimeter data. Before this was done, the annual astronomical tidal contribution, $\mathbf{S_a}$, was estimated from the OT predictions and removed, as it includes seasonal effects that to a large extent are already accounted for in the IB correction (Pugh and Woodworth, 2014). All TG observations were corrected for the IB effect using Wunsch and Stammer (1997) with respect to a reference value of 1011.4 mbar (Woodworth et al., 2012). At HAMM TG, no local pressure observations were available, and pressure data from a nearby meteorological station were used instead. Those pressure observations were obtained from the eKlima database of the Norwegian Meteorological Institute, at https://eklima.met.no/.

### 2.3. CryoSat-2 tide gauges

Treating CS2 like a 369-day repeat altimeter would only give four observations per point for the 2010–2014 period. Consequently, we consider a different approach. We established 45 × 45 km boxes around each TG containing CS2 observations and forming "CS2 tide gauges" (CS2TGs), shown in Figs. 7 and 8. The CS2TGs were positioned around each TG depending on topography, such that they cover as much marine area as possible, but still keep a minimum distance of 0.2° between the TG and the edge of the CS2 tide-gauge (CS2TG) box. The 45-km distance was chosen based on the geodetic orbit and temporal resolution of CS2. A CS2 orbit repetition cycle includes 13 sub-cycles. To include one CS2 repetition cycle (observations over a whole year, not only seasonal tracks) in our CS2TG box, and taking the CS2 across-track distance of 8 km at the equator into account, we need a 100 × 100 km CS2TG box. For Norway, with a mean latitude of 65°, we end up with a 45-km box. At TGs close to the open ocean, more than enough observations were available within the CS2TGs, while a more critical situation was found at TGs located inside fjords. Fig. 2 shows the data situation within the CS2TGs at three TGs to the open ocean (BODO, KABE, and VIKE), as well as three TGs well inside fjords (OSLO, OSCA, VIKE). We take the 45-km distance to be a trade-off between having enough points to have a sufficient temporal resolution for deriving meaningful statistics, as well as being close enough such that CS2 still observes the same ocean signal as the TG (see also Section 2.4).

As mentioned in Section 2.1, we did not downsample the 20 Hz observations to 1 Hz. This is normally done by the

Table 2
CS2TGs at 22 Norwegian TGs.

| Tide-gauge | Tide-gauge code | No. obs. | No. obs. ∈ [−1, 1] m DTU15 | Used no. obs. | $t > t_{(\alpha/2,f)}$ [%] | No. tracks |
|---|---|---|---|---|---|---|
| Vardø | VARD | 6111 | 5710 | 4639 | 19 | 93 |
| Honningsvåg | HONN | 6546 | 4457 | 3498 | 22 | 79 |
| Hammerfest | HAMM | 5611 | 3669 | 2947 | 20 | 90 |
| Tromsø | TROM | 2438 | 587 | 494 | 16 | 36 |
| Andenes | ANDE | 8023 | 7662 | 6318 | 18 | 95 |
| Harstad | HARS | 6010 | 4031 | 3034 | 25 | 83 |
| Kabelvåg | KABE | 7319 | 6639 | 5256 | 21 | 92 |
| Bodø | BODO | 7463 | 5909 | 4680 | 21 | 85 |
| Rørvik | RORV | 7940 | 7060 | 5410 | 23 | 102 |
| Mausund | MAUS | 7489 | 6678 | 5214 | 22 | 94 |
| Trondheim | TRON | 4826 | 1940 | 1495 | 23 | 56 |
| Heimsjø | HEIM | 5018 | 3030 | 2458 | 19 | 89 |
| Kristiansund | KRIN | 9949 | 9125 | 7422 | 19 | 97 |
| Ålesund | ALES | 9653 | 7352 | 5869 | 20 | 89 |
| Måløy | MALO | 9246 | 6411 | 5321 | 17 | 70 |
| Bergen | BERG | 5820 | 3962 | 3157 | 20 | 74 |
| Stavanger | STAV | 9365 | 8433 | 6731 | 20 | 94 |
| Tregde | TREG | 7695 | 7453 | 6118 | 18 | 92 |
| Helgeroa | HELG | 7496 | 7121 | 5824 | 21 | 92 |
| Oscarsborg | OSCA | 2346 | 1747 | 1377 | 21 | 49 |
| Oslo | OSLO | 493 | 255 | 224 | 12 | 21 |
| Viker | VIKE | 7407 | 6219 | 4960 | 20 | 67 |

Please cite this article in press as: Idžanović, M., et al. Coastal sea level from CryoSat-2 SARIn altimetry in Norway. Adv. Space Res. (2017), http://dx.doi.org/10.1016/j.asr.2017.07.043

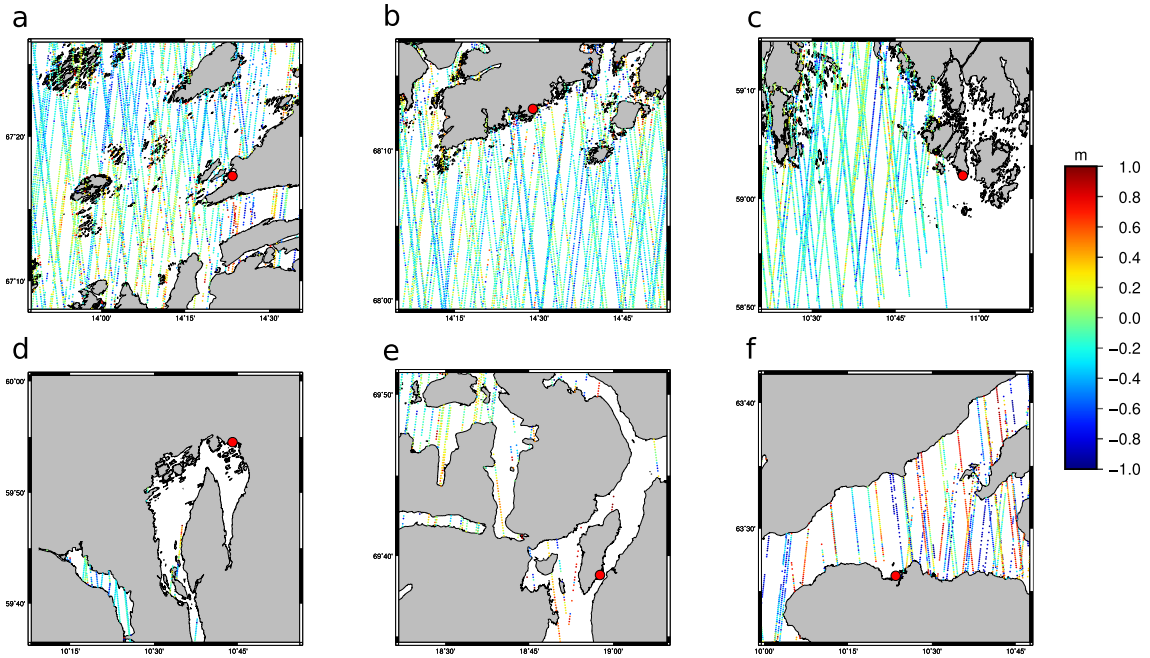


Fig. 2. SLAs in CS2TGs at (a) BODO, (b) KABE, (c) VIKE, (d) OSLO, (e) OSCA, and (f) TRON. The red dots denote the TGs. Note that OSLO and VIKE TGs are situated just outside the SARIn geographical mode mask (Fig. 1a), giving less observations in parts of the respective CS2TGs.

space agencies using iterative editing and averaging, which will increase the data accuracy. Since the CS2 observations within a track are sampled very closely in time (all CS2 observations within a track would be assigned the same TG observation), we averaged all 20 Hz observations within a track, and linearly interpolated the TG observations to the time of the averaged CS2 observations using a nearest-neighbor approach. On average, 79 CS2 tracks were available in each CS2TG. In addition to standard deviations of differences between CS2TG and TG time series, Spearman's (distribution-free) rank correlation coefficient, $\rho$, was computed. Spearman's $\rho$ is a non-parametric method for detecting relations between two variables. Non-parametric methods are relatively insensitive to outliers, and do not assume that the observations are normally distributed (Hollander et al., 2013). It is a slightly more conservative value than the well-known Pearson correlation coefficient.

Table 2 summarizes the processing results for the 22 CS2TGs. In some cases, there are slight differences of the resulting number of valid SLAs depending on whether standard or local corrections are applied. Consequently, the three rightmost columns in Table 2 are average values from both cases.

### 2.4. Range and geophysical corrections

As opposed to the Jason-2, Envisat, and SARAL/AltiKa altimetry satellites, CS2 does not carry a radiometer. Therefore, the corrections for the wet (WET) and dry (DRY) tropospheric refraction must be derived using models, where CS2 uses the ECMWF model (Dee et al., 2011). CS2 is furthermore a single-frequency altimeter, hence the correction for the ionospheric refraction (IONO) is also provided by a model, i.e., the GPS-based global ionospheric model (GIM) (Komjathy and Born, 1999). In general, these corrections are believed to be only slightly less accurate than the instrument-derived corrections applied on conventional altimeters (Andersen and Scharroo, 2011).

The CS2 dynamic atmosphere correction (DAC) consists of a high-frequency part provided by MOG2D (Carrère and Lyard, 2003) and a low-frequency part, IB, provided by ECMWF ($IB_{ECMWF}$). The tide correction consists of OT, nodal tide (NT), ocean tide loading (OTL), solid Earth tide (SET), and pole tide (PT). The CS2 OT correction ($OT_{FES2004}$) is provided by the FES2004 global OT model (Lyard et al., 2006), which is similar to those used in conventional satellites. See Table 3 for an overview of applied corrections.

Fig. 3b shows the signal standard deviations of the range and geophysical corrections in all CS2TGs. The DRY, WET, and IONO range corrections show smooth correction curves along the coast, with values of less than 6 cm, while NT, OTL, SET, and PT show values of ~8 cm or less. We note that by far the largest contributors to the corrections are OT (up to ~80 cm at the northernmost TGs) and IB (~12 cm), in accordance with Andersen and Scharroo (2011). Here, $OT_{FES2004}$ and $IB_{ECMWF}$ are the standard OT and IB corrections for CS2. Fig. 3a shows the percentage of CS2 observations not having a FES2004 OT correction assigned to them within the CS2TGs. In accordance with the findings of Abulaitijiang et al. (2015), there is a considerable amount of global OT values missing at TGs well inside fjords, particularly at TROM, TRON, and OSLO. Looking at Fig. 1b we note that these TGs are outside the coverage of the

Please cite this article in press as: Idžanović, M., et al. Coastal sea level from CryoSat-2 SARIn altimetry in Norway. Adv. Space Res. (2017), http://dx.doi.org/10.1016/j.asr.2017.07.043

Table 3
Range and geophysical corrections for CS2 (Webb and Hall, 2016), SARAL/AltiKa, Envisat/C, and Jason-2 (Scharroo et al., 2013).

| Correction | Observation or model for | | | |
|---|---|---|---|---|
| | CS2 | SARAL/AltiKa | Envisat/C | Jason-2 |
| Dry troposphere | ECMWF | ECMWF | ECMFW | ECMWF |
| Wet troposphere | ECMWF | Radiometer | Radiometer | Radiometer |
| Ionosphere | GIM | GIM | GIM | Dual frequency |
| Inverse barometric correction | ECMWF | ECMWF | ECMWF | ECMWF |
| High-frequency atmospheric variations | MOG2D | MOG2D | MOG2D | MOG2D |
| Ocean tide | FES2004 | FES2004 | FES2004 | FES2004 |
| Ocean tide loading | FES2004 | FES2004 | FES2004 | FES2004 |
| Long-period tide | FES2004 | FES2004 | FES2004 | FES2004 |
| Solid Earth | Cartwright/Edden | Cartwright/Edden | Cartwright/Edden | Cartwright/Edden |
| Pole tide | Wahr | Wahr | Wahr | Wahr |
| Mean sea surface | DTU15 MSS | DTU13 MSS | DTU13 MSS | DTU13 MSS |
| Bias | 1.38 m[a] | – | – | – |

[a] Includes the difference between TOPEX and WGS84 ellipsoids as well as the SARIn range bias, which must be applied to baseline B products (Scagliola and Fornari, 2017).

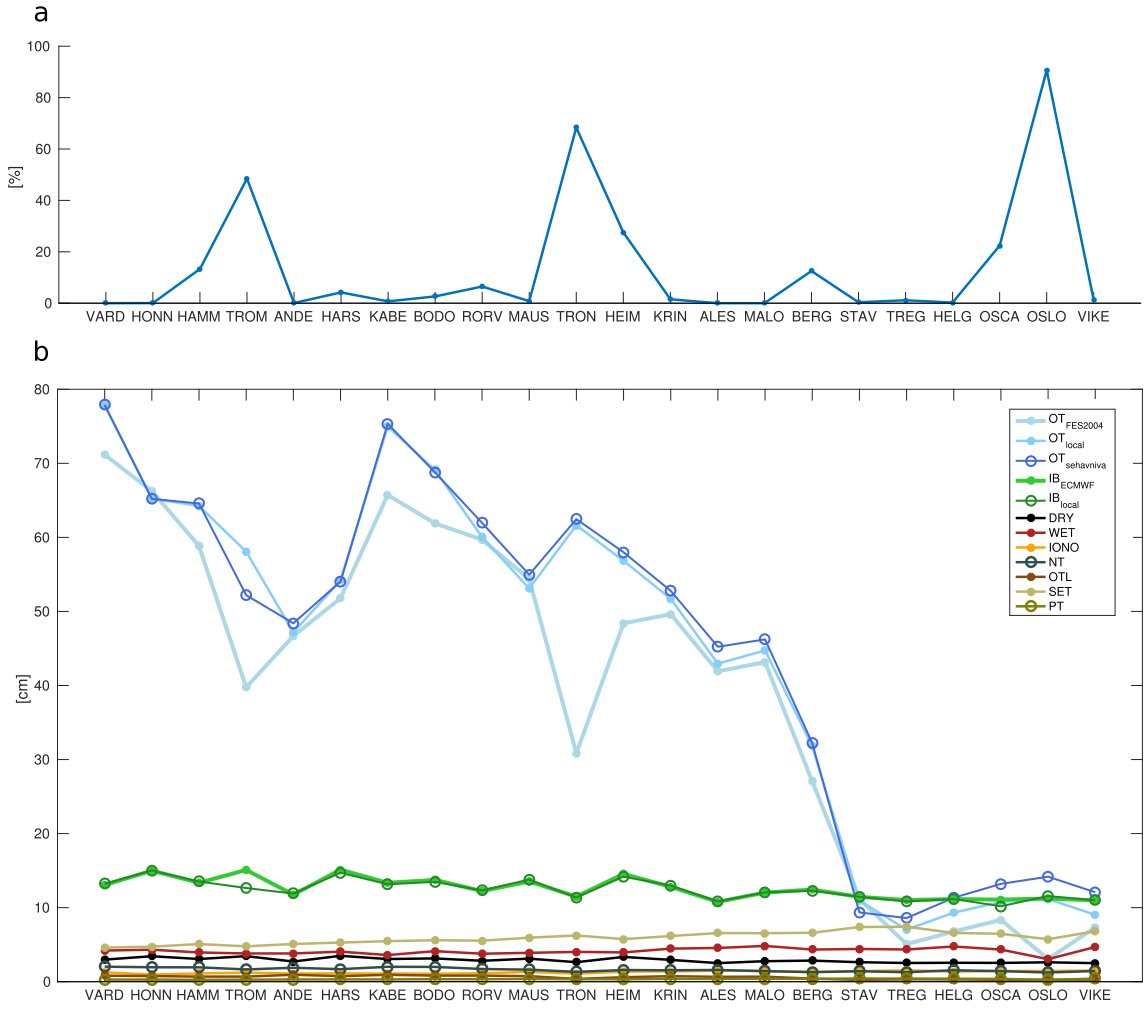


Fig. 3. (a) Percentage of CS2 observations missing the FES2004 OT correction within CS2TGs. (b) Signal standard deviations of CS2 range and geophysical corrections within CS2TGs.

FES2004 grid, where the standard OT correction is consequently set to zero.

The substitution of standard corrections with locally refined corrections in the post-processing of coastal altimetry data has proven to be a successful strategy (e.g., Bouffard et al., 2011; Birol et al., 2017). The availability of local OT predictions and pressure data (Section 2.2) allowed us to substitute the standard OT and IB correc-

tions ($OT_{FES2004}$ and $IB_{ECMWF}$) with $OT_{local}$ and $IB_{local}$ derived from TGs. The substituted corrections are termed local corrections in the following. Fig. 3b reveals that the $IB_{ECMWF}$ and $IB_{local}$ curves are very similar. Since the IB is the low-frequency part of the total DAC correction, we did not expect in situ pressure observations to show large differences to ECMWF model pressure. The agreement between the ECMWF model pressure and the locally observed pressure suggests that the ECMWF model pressure is sufficiently accurate for the areas considered along the Norwegian coast.

However, we observe a larger difference between the $OT_{FES2004}$ and $OT_{local}$ curves. As expected, the most prominent differences appear at TGs where a considerable amount of FES2004 OT values is missing. There is also a larger discrepancy between standard and local OT signal at KABE, which mainly contains valid FES2004 OT values. A possible explanation is that FES2004 does not fully capture the complex OT signal in that area.

To support our CS2TG choice we explored the OT signal variability within the CS2TGs. This was done by computing OT corrections for the CS2TGs using the tide and sea-level web service of NMA ($OT_{sehavniva}$, http://www.kartverket.no/sehavniva/). Using $OT_{sehavniva}$, each CS2 observation is assigned an individual OT correction, determined by a spatial interpolation of OT using site-specific scaling factors and time delays to observations from the nearest permanent and temporary TGs. This contrasts $OT_{local}$, which simply assigns the TG OT prediction value to all observations within the CS2TG. An agreement of $OT_{sehavniva}$ with $OT_{local}$ thus suggests that the CS2TG indeed covers an area showing similar ocean variability.

In Fig. 3b we note that $OT_{sehavniva}$ and $OT_{local}$ generally agree well, especially in areas with a large amount of observations. It suggests that the CS2TGs represent areas that are compatible with the TGs. Larger discrepancies are seen in TROM, OSCA, and OSLO, i.e., at TGs that are already problematic due to few CS2 observations (Figs. 2d–f), and where the CS2TG approach is not ideal.

### 2.5. Conventional altimeter data

Jason-2, Envisat, and SARAL/AltiKa 1 Hz altimetry data were extracted from the radar altimeter database system (RADS) (Scharroo et al., 2013), with standard corrections applied. Due to the orbit configuration of Jason-2, only data up to 66°N are available. For each altimeter, the two nearest tracks to the TG were considered. For consistency with the CS2TGs, for each track, a $45 \times 45$ km box was centered on the TG and then shifted westwards by 0.1°. Next, all altimeter observations within the box were averaged. In the following, when referring to conventional altimetry sites, it is the average location of the observations within the box that is meant. For some TGs (HELG, TREG, MALO, TROM), the search radius had to be extended to find a valid track. The time period of the conventional altimetry data was adapted as far as possible to the CS2 time period. For Jason-2, its entire 2010–2016 period was used, while for Envisat only the period between 2010 and 2012 (phase C) was used, where the satellite was in a 30-day repeat orbit. For SARAL/AltiKa the period after 2013 could be used. We are aware of the fact that SARAL/AltiKa is not strictly a conventional altimeter, as it has a smaller footprint and lower noise due to its lower altitude, antenna pattern, and Ka-band frequency (Verron et al., 2015). In this study, however, we use the term conventional altimetry only to distinguish pulse-limited altimetry from SAR altimetry.

The number of observations from the conventional altimeters will generally not correspond with the expected number of observations considering the number of repeats for each altimeter time period. This is due to the averaging box and that the RADS data are not resampled to reference tracks. For Jason-2 ~200 observations were averaged, while for SARAL/AltiKa and Envisat ~30 and ~15 observations were averaged, respectively. Furthermore, TGs that lie further inside fjords than TGs closest to the open ocean, have been assigned the same altimeter tracks as the latter. This is because the tracks around the open-ocean TGs are also the closest to the TGs inside fjords. Consequently, (HARS, ANDE), (TRON, HEIM, MAUS), and (OSLO, OSCA, VIKE) are compared with the same altimeter tracks. In addition, at VIKE, roughly the same site was chosen for each track in case of Envisat and SARAL/AltiKa, as the two tracks are crossing there. For consistency, the SSHs were extracted from RADS using the same geophysical corrections as for CS2 (Table 3).

Several experimental coastal altimetry projects exist, such as Jason-2/PISTACH (Mercier et al., 2008), Envisat/COASTALT (Dufau et al., 2011), multi-mission/CTOH (Roblou et al., 2011), or the recent coastal altimetry product based on SARAL/AltiKa (Valladeau et al., 2015). Some of these are distributed through AVISO. In their study along the Norwegian coast, Ophaug et al. (2015) found that tailored coastal altimetry products based on Jason-2 and Envisat offered only marginal improvements over the conventional observations, thus we did not consider coastal altimetry products in this study.

## 3. Results

### 3.1. Comparison of CryoSat-2 with tide gauges along the Norwegian coast

Fig. 4 shows time series of SLAs from CS2TGs and sea level from TGs between 2010 and 2014 at 22 sites, using standard CS2 corrections. Generally, the two time series agree well, with a mean standard deviation of differences of 16.0 cm and a mean correlation of 61%. Fig. 5 shows the same time series using local CS2 corrections. These two time series agree better than the ones in the standard case, with a mean standard deviation of differences of 12.2 cm and a mean correlation of 68%. The time series at TGs close to the open ocean (e.g., VARD, ANDE,

Please cite this article in press as: Idžanović, M., et al. Coastal sea level from CryoSat-2 SARIn altimetry in Norway. Adv. Space Res. (2017), http://dx.doi.org/10.1016/j.asr.2017.07.043

STAV, VIKE) agree better than the time series at land-confined TGs (e.g., TROM, TRON, HEIM, BERG).

Fig. 6 shows standard deviations of differences and correlations between the TGs and CS2, using both standard and local corrections. Using standard corrections (solid lines in Fig. 6), the standard deviations of differences are 20 cm or more at land-confined TGs (e.g., TROM, TRON, HEIM, BERG), while TGs to the open ocean (e.g., VARD, ANDE, STAV, VIKE) have standard deviations of differences of 9 cm or less. Related behavior is seen for correlations in Fig. 6b. A comparison of curves in Figs. 3a and 6a reveals that deviating locations are due to missing $OT_{FES2004}$ values.

Using local corrections (dashed lines in Fig. 6), we observe an improvement in standard deviations of differences at 19 out of 22 TGs (exceptions are ALES, MALO, and OSCA). Local corrections yield an average improvement of ~24% in standard deviations of differences and ~12% for correlations. Applying local corrections, large decreases in standard deviations of differences are observed at HAMM, KABE, BODO, RORV, TRON, and HEIM, i.e., at TGs that are both land-confined and to the open ocean. Among land-confined TGs with few observations, TRON and TROM show large drops in standard deviations of differences, and the correlation increases. These CS2TGs are characterized by a small number of valid observations. Among TGs to the open ocean with many observations, BODO, KABE, and VIKE show significant drops in standard deviations of differences and increased correlation. This indicates a gain in determining the OT correction by a local approach.

### 3.2. Comparison of conventional altimetry with tide gauges along the Norwegian coast

Figs. 7 and 8 show standard deviations of differences and correlations between time series of SLAs from the conventional altimetry missions (Envisat, SARAL/AltiKa, and Jason-2) and sea level from TGs. In addition, the CS2TGs are shown, to give an overview of the spatial distribution of the data used in this study.

We first note that the mean distance from the conventional altimetry sites and TGs is 53 km, which agrees with the findings of Ophaug et al. (2015). Due to the lower spa-

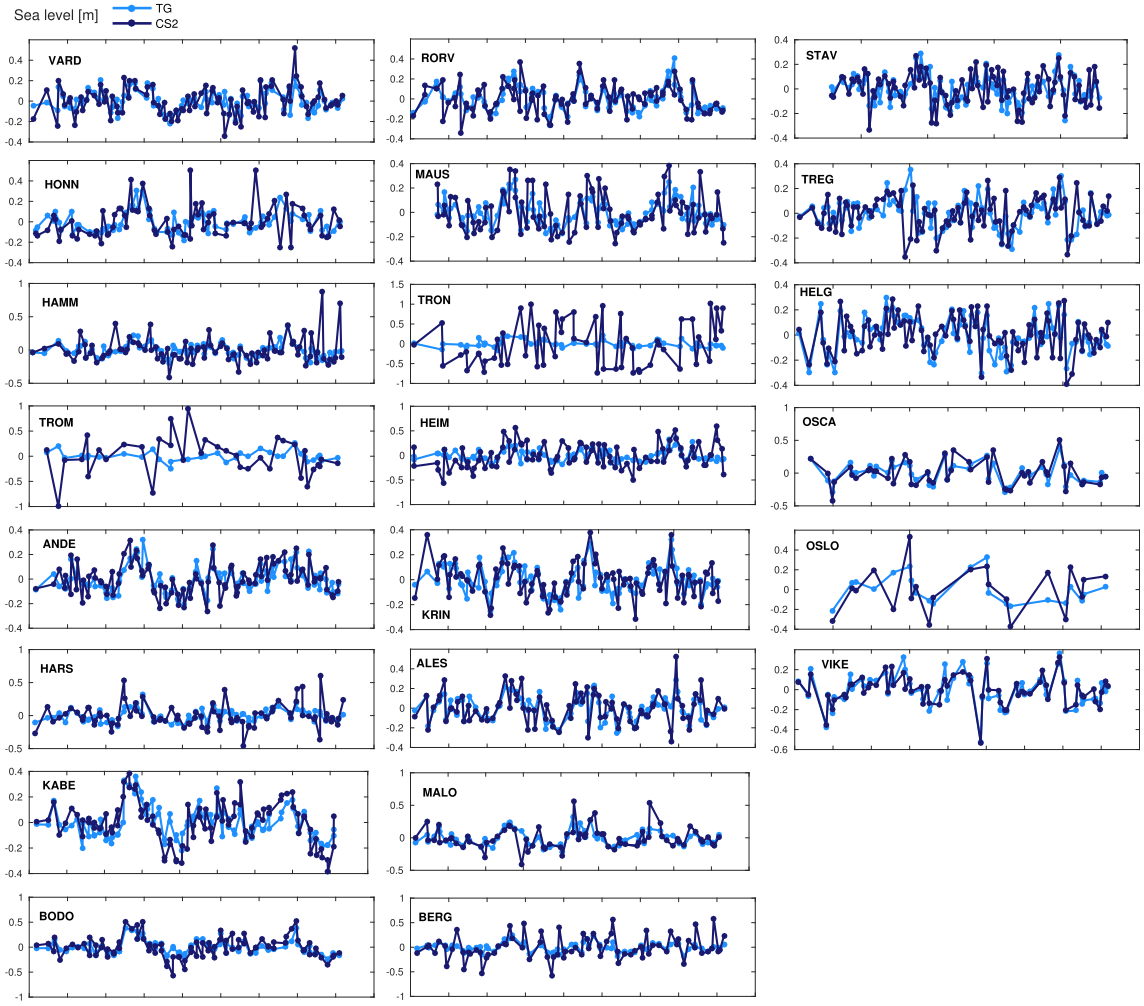


Fig. 4. Comparison of CS2TG SLAs with TG sea level using standard corrections.

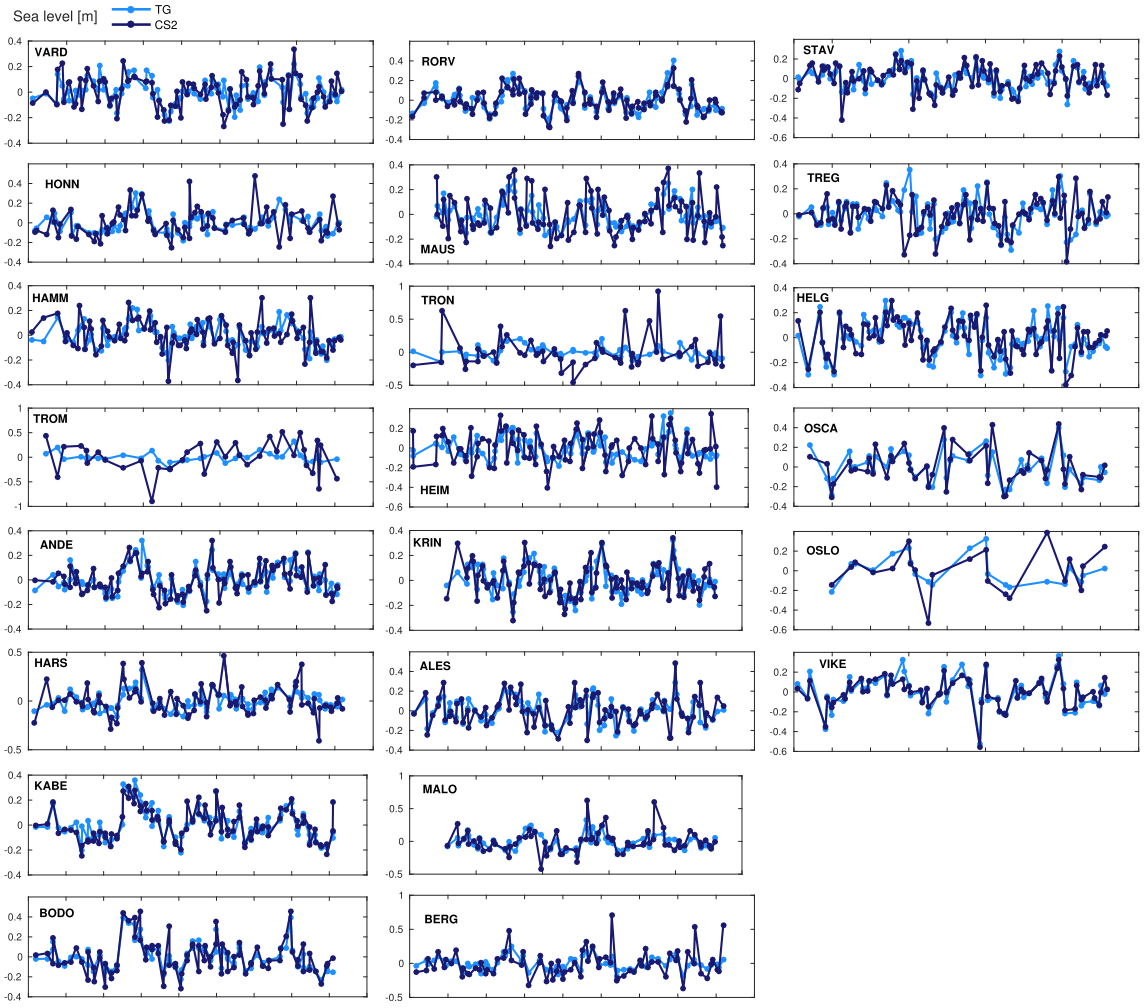


Fig. 5. As Fig. 4, but using local corrections.

tial resolution of Jason-2, its sites are typically little further from the CS2TGs than those from Envisat and SARAL/AltiKa, with a mean distance of 71 km. The mean distance for Envisat is 50 km and for SARAL/AltiKa 45 km. The largest distance between all conventional altimeters and TGs is at OSLO. Although the CS2TG at OSLO has valid observations well within the 45-km box, it is an area where CS2 also struggles due to few observations as a result of the geographical mode mask border (see Fig. 1a).

All conventional altimeters perform similarly. As with CS2, there are variations between standard deviations and correlations at different TGs. Envisat shows the largest standard deviation of differences of 18.9 cm at KRIN. Both Envisat and SARAL/AltiKa show the smallest standard deviation of differences of 5.1 cm at TROM and ANDE, respectively. Regarding correlations, Envisat shows the smallest correlation of 10% at TROM, while SARAL/AltiKa shows the largest correlation of 90% at TROM.

There is a tendency that correlation decreases and standard deviation of differences increases with increasing distance to the TG for all altimeters. These results suggest that the agreement of conventional altimetry with the TGs improves from Jason-2 through Envisat to SARAL/Altika. As mentioned earlier, the smaller footprint of SARAL/AltiKa makes it particularly suitable for coastal applications, and explains it outperforming Envisat and Jason-2. However, we note that at TGs where both altimeter sites are similarly close to the TG, the performance of the individual sites sometimes varies without obvious reason. The good performance at TGs that use common altimetry tracks (HARS, TRON, HEIM) can be seen as an indicator that the CS2TGs were not chosen too large (Section 2.3).

Similar to CS2, the mean correlation of the conventional altimeters with the TGs is 60%, but with a slightly lower mean standard deviation of differences of 11 cm. However, if the land-confined CS2TGs (e.g., TROM, TRON, HEIM, BERG), are omitted in the analysis, the CS2TGs show a mean correlation of 69%, and a mean standard deviation of differences of 12 cm (with standard corrections), and a mean correlation of 74%, and a mean standard deviation of differences of 10 cm (with local corrections). Practically

Please cite this article in press as: Idžanović, M., et al. Coastal sea level from CryoSat-2 SARIn altimetry in Norway. Adv. Space Res. (2017), http://dx.doi.org/10.1016/j.asr.2017.07.043

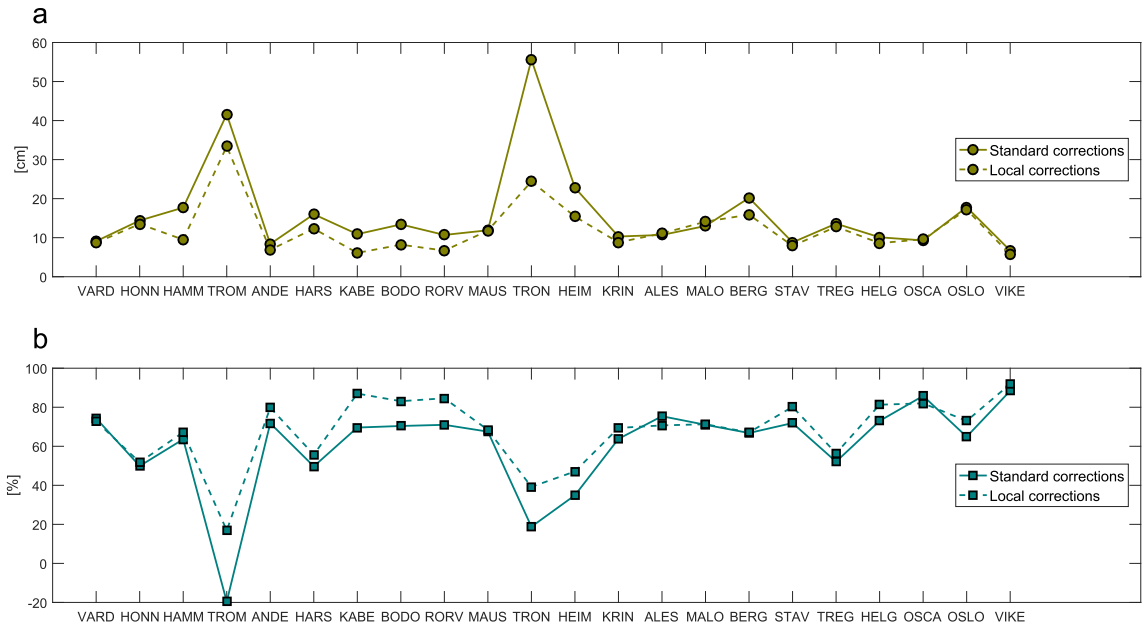


Fig. 6. Comparison of CS2 with TGs using standard and local OT and IB corrections, in terms of (a) standard deviations of differences and (b) correlations. The TGs are ordered such that the northernmost TG appears first on the left-hand side of the horizontal axis, moving southward along the Norwegian coastline.

the same results are obtained from the CS2TGs if those that use common conventional altimetry tracks are left out (HARS, TRON, HEIM, OSLO, OSCA). This suggests that, if the problematic CS2TGs are set aside, there is an improvement with CS2 as it gets closer to the coast than conventional altimeters.

As of yet, not many validation studies of CS2 SAR performance along coasts exist. Fenoglio-Marc et al. (2015) compared CS2 with the Helgoland island TG in the German Bight, and found standard deviations of differences of 6.6 cm for pseudo-LRM data and 7.7 cm for SAR-mode data (with higher range precision than our degraded SARIn observations) at a maximum distance of 20 km from the TG. As opposed to our CS2 data, a sea-state bias correction from the RADS hybrid model was applied. In a recent validation of a global CS2 geophysical ocean product (based on LRM and pseudo-LRM data), Calafat et al. (2017) found standard deviations of differences to 22 TGs spread across the globe of 7.1 cm. They also compared Jason-2 with the same set of TGs, and found a similar standard deviation of differences of 7.3 cm. Our results show a similar or better agreement (at favorable TGs), despite the complexity of the study area and the application of the degraded SARIn mode data.

In general, the observed discrepancies between altimetric SLAs and TG sea level are due to instrument noise and the fact that the altimeter and the TG sample slightly different ocean signals (Calafat et al., 2017). The latter aspect can be particularly problematic at northern high latitudes, where the baroclinic Rossby radius is expected to be smaller than 10 km (Chelton et al., 1998). At TGs where coastal or other complex ocean processes are expected to be dominant (e.g., KABE, TROM, TRON, HEIM, BERG), the observed differences between altimetry and TGs will be larger.

Furthermore, the derived time series from CS2 and the conventional altimeters are not strictly consistent with respect to the sampling interval. We practically compare instantaneous sea level observations and do not perform any temporal averaging of the altimetry observations exceeding the individual passes. However, as noted by Calafat et al. (2017), the comparison of instantaneous sea-level observations sampled with a certain periodicity is still consistent.

Finally, we emphasize a few aspects which make the conditions for the CS2TGs more challenging than for the conventional altimeters. First, the SLA observations from CS2 are taken from multiple tracks within the CS2TG. Potential errors in the MSS will appear as SLA offsets between the tracks. This, in turn, could appear as an SLA error in the comparison with the TG, making it a bigger challenge for CS2 than for conventional repeat-altimetry (Calafat et al., 2017). It becomes a serious issue close to the coast because of the interpolation error in the MSS. It is larger in the coastal areas due to missing observations and simple extrapolation. It could also be a problem for the conventional altimeters, although less so because the observations are much more concentrated in space. In addition, the conventional altimetry sites are more to the open ocean, where Smith and Scharroo (2009) found that current MSS models did not introduce significant errors in the SLAs.

Please cite this article in press as: Idžanović, M., et al. Coastal sea level from CryoSat-2 SARIn altimetry in Norway. Adv. Space Res. (2017), http://dx.doi.org/10.1016/j.asr.2017.07.043

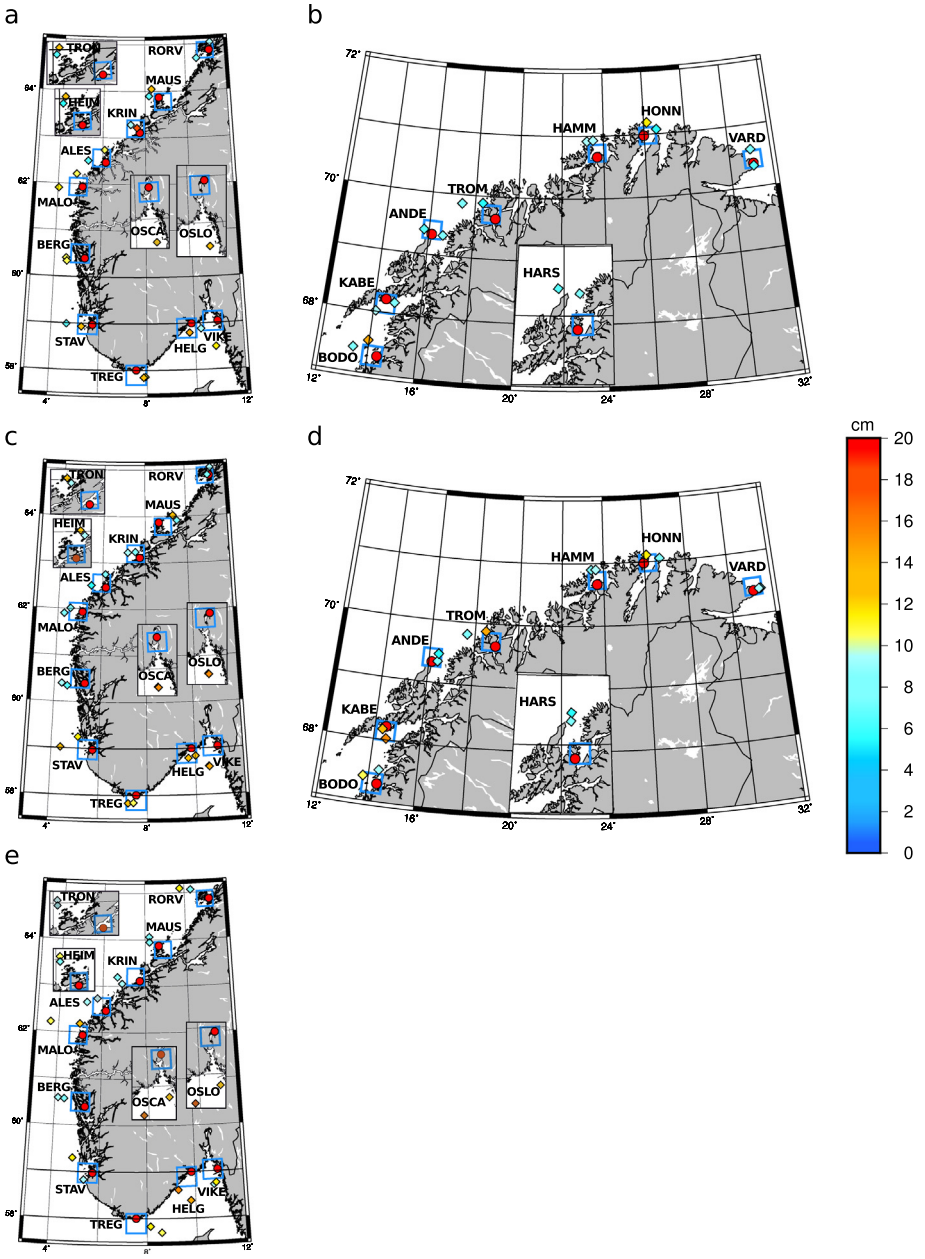


Fig. 7. TGs (red dots), CS2TGs (blue boxes) and conventional altimetry (diamond markers) along the Norwegian coast. The diamond markers, placed in the average location of the observations within the boxes, show standard deviations of differences between conventional altimetry and the 22 TGs; Envisat (a) south of 66°N, (b) north of 66°N, SARAL/AltiKa (c) south of 66°N, (d) north of 66°N, and Jason-2 (e) south of 66°N.

Second, the conventional altimetry data from RADS have robust editing criteria, and we expect these data to be of higher quality than the CS2 SARIn-mode data. The SLAs from CS2 are based on preliminary processing and data screening. The DTU Space retracking system is experimental and under development. Our editing of the CS2 degraded SARIn data is crude. A considerable amount of valid data points did not pass the editing, and reveals that CS2 targets along the Norwegian coast are noisy and prone to instrumental errors. An example of the latter is that when CS2 passes a fjord with steep mountains on either side, it will track its own noise instead of the fjord surface. Also, we have seen that a large amount of the CS2 observations well inside fjords lack OT corrections, which can be saved in post-processing by considering local OT corrections.

## 4. Summary and conclusions

We have performed an initial validation of CS2 along the Norwegian coast, over areas previously not monitored by conventional altimetry. The validation is done by comparing CS2 with in situ observations at 22 TGs. As pointed out by Calafat et al. (2017), CS2 has been shown to be as suitable for oceanography as are conventional altimeters. CS2 was designed for cryospheric and geodetic studies

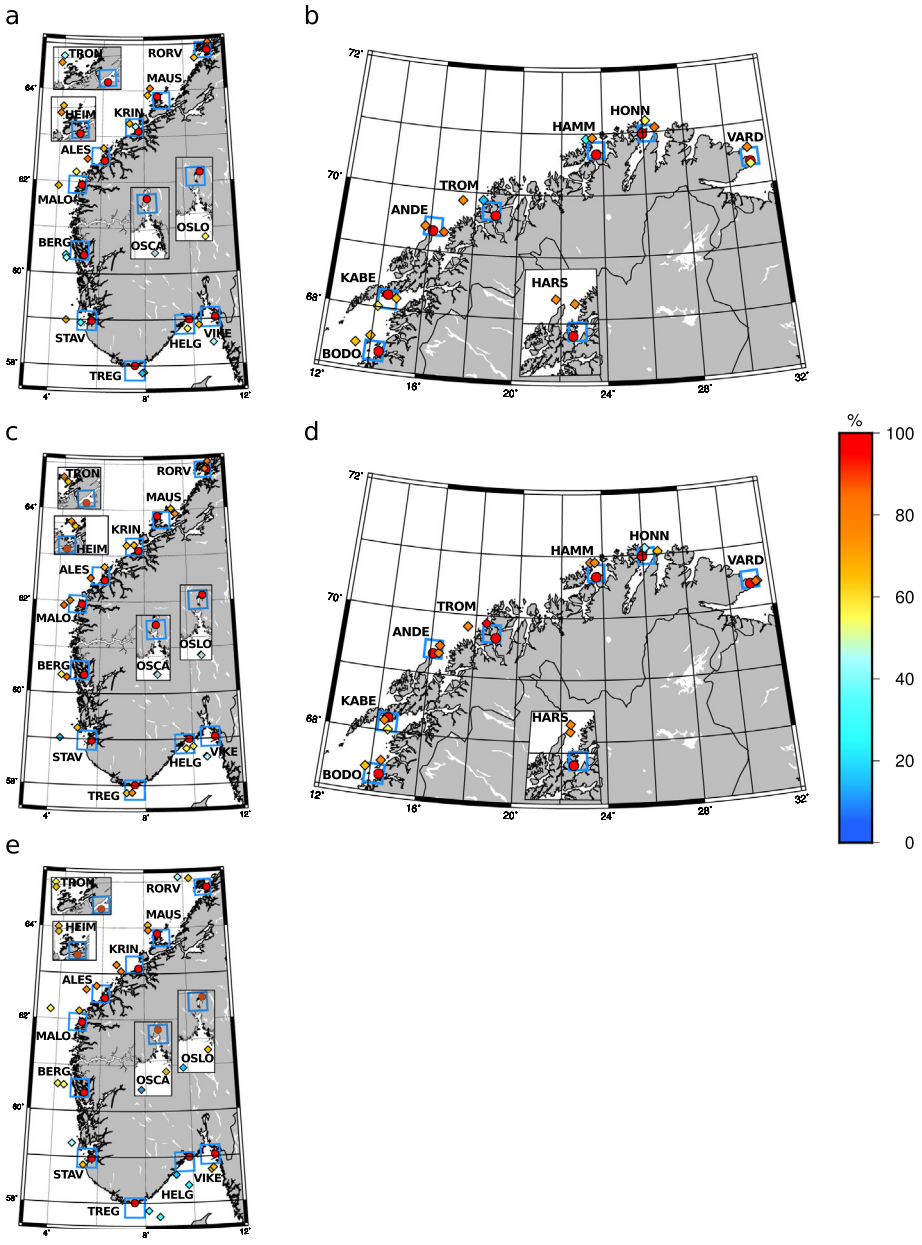


Fig. 8. As Fig. 7, but here the diamond markers show temporal correlations of conventional altimetry with the 22 TGs; Envisat (a) south of 66°N, (b) north of 66°N, SARAL/AltiKa (c) south of 66°N, (d) north of 66°N, and Jason-2 (e) south of 66°N.

which require a high spatial resolution (as opposed to studies of ocean dynamics, which require a high temporal resolution).

The entire Norwegian coast falls into the CS2 SARIn mode mask, but the phase information was not applied to these observations at the time of processing. Thus, the considered observations are a kind of degraded SARIn observations, with a noisier signal due to less waveforms that are averaged in SARIn mode than in pure SAR mode. The geodetic orbit of CS2 gives a denser spatial coverage than conventional repeat-altimetry, with an average of 4208 20 Hz SLAs within a $45 \times 45$ km area around TGs, i.e., CS2TGs. The CS2TGs are both close to the open ocean and land-confined/inside fjords. We find that the $45 \times 45$ km box is a good compromise between having a sufficient number of observations to derive meaningful statistics, and still cover a small enough area such that the OT variability within the CS2TGs is relatively similar to the OT variability at TGs.

Close to the coast, the validity of the range and geophysical corrections are of particular importance. By inspection within the CS2TGs, we confirmed that the OT and IB corrections are the largest signal contributors to the corrections, with the former being decisive along the Norwegian coast, because the OT range is large. The OT correction was missing at several land-confined TGs, so we investigated how local corrections from pressure observations and OT predictions perform within the CS2TGs. The IB correction did not change significantly when using local pressure instead of ECMWF model pressure, but

Please cite this article in press as: Idžanović, M., et al. Coastal sea level from CryoSat-2 SARIn altimetry in Norway. Adv. Space Res. (2017), http://dx.doi.org/10.1016/j.asr.2017.07.043

the OT correction, as expected, had a significant impact. Thus, we compared CS2TGs with the TGs using both standard and local corrections.

Using standard corrections, the standard deviation of differences and correlation over all 22 TGs is 16 cm and 61%, respectively. Using local corrections, these values are 12.2 cm and 68%. We note a considerable improvement at CS2TGs that are missing standard OT corrections and have few CS2 observations, but also at reliable CS2TGs with many observations. The latter suggests a gain by a local approach to determining the OT correction.

To compare these results with conventional altimetry, the same analysis with 22 TGs was done using data from three conventional altimetry missions, Envisat, SARAL/AltiKa, and Jason-2. They show mean standard deviations of differences of 10.0 cm, 10.6 cm, and 11.0 cm, and mean correlations of 58%, 64%, and 56%, respectively. There is a tendency that standard deviation of differences increases and correlation decreases with increasing distance to the TG for all altimeters.

If the problematic CS2TGs are left out of the analysis, thus making CS2 more comparable to the conventional altimeters, the standard deviation of differences and correlation over all TGs is 12 cm and 69% (with standard corrections), and 10 cm and 74% (with local corrections).

These results confirm that CS2 SARIn-mode observations, even with their degraded range precision and without the phase information, are of comparable quality to those from conventional altimetry. A next step could be a more elaborate modeling of the DAC (including high-frequency atmospheric variations, see, e.g., Bouffard et al. (2011) or Woodworth and Horsburgh (2011)), and an improved WET correction using the national GNSS network (Obligis et al., 2011). Future improvements of the retracker system (e.g., inclusion of the phase information in the processing, giving pure SARIn observations) and the investigation of other retrackers may mitigate noise. A more elaborate statistical editing of the data, such as that employed by Nielsen et al. (2015), could also provide a larger amount of valid observations.

We have used the CS2 ice baseline B processor in this study. It has later been replaced by the ice baseline C processor (Bouffard et al., 2015). A tailored ocean processing of CS2, the CryoSat Ocean Processing (COP) baseline C, will be released in 2017 (Bouffard et al., 2016). In future coastal applications of CS2, these baselines should be considered.

The main improvement of CS2 is due to the smaller SAR footprint, enabling observations closer to the coast than conventional altimeters. As such, this study has implications for next-generation SAR altimetry missions such as Sentinel-3 and Jason-CS/Sentinel-6.

## Acknowledgments

We would like to thank K. Breili at NMA, for providing TG data and helpful comments. ESA and RADS are acknowledged for providing CryoSat-2 and other altimetry data, respectively. The manuscript was considerably improved through constructive comments from two anonymous reviewers, which are gratefully acknowledged. O.B. Andersen was supported by the ESA's GOCE++DYCOT project. This study is part of the Norwegian University of Life Science's GOCODYN project, supported by the Norwegian Research Council under project number 231017.

## References

Abulaitijiang, A., Andersen, O.B., Stenseng, L., 2015. Coastal sea level from inland CryoSat-2 interferometric SAR altimetry. Geophys. Res. Lett. 42 (6), 1841–1847. http://dx.doi.org/10.1002/2015GL063131.

Andersen, O.B., Knudsen, P., Stenseng, L., 2015. The DTU13 MSS (mean sea surface) and MDT (mean dynamic topography) from 20 years of satellite altimetry. In: IAG Symposia. Springer, Berlin Heidelberg. http://dx.doi.org/10.1007/1345_2015_18.

Andersen, O.B., Scharroo, R., 2011. Range and geophysical corrections in coastal regions: and implications for mean sea surface determination. In: Vignudelli, S. et al. (Eds.), Coastal Altimetry. Springer, Berlin Heidelberg, pp. 103–145. http://dx.doi.org/10.1007/978-3-642-12796-0_5.

Armitage, T.W.K., Davidson, M.W.J., 2014. Using the interferometric capabilities of the ESA CryoSat-2 mission to improve the accuracy of sea ice freeboard retrievals. IEEE Trans. Geosci. Rem. Sens. 52 (1), 529–536. http://dx.doi.org/10.1109/TGRS.2013.2242082.

Birol, F., Fuller, N., Lyard, F., Cancet, M., Niño, F., Delebecque, C., Fleury, S., Toublanc, F., Melet, A., Saraceno, M., Léger, F., 2017. Coastal applications from nadir altimetry: example of the X-TRACK regional products. Adv. Space Res. 59 (4), 936–953. http://dx.doi.org/10.1016/j.asr.2016.11.005.

Bouffard, J., Roblou, L., Birol, F., Pascual, A., Fenoglio-Marc, L., Cancet, M., Morrow, R., Ménard, Y., 2011. Introduction and assessment of improved coastal altimetry strategies: case study over the Northwestern Mediterranean Sea. In: Vignudelli, S. et al. (Eds.), Coastal Altimetry. Springer, Berlin Heidelberg, pp. 297–330. http://dx.doi.org/10.1007/978-3-642-12796-0_1.

Bouffard, J., Manner, R., Brockley, D., 2015. CryoSat-2 Level 2 Product Evolutions and Quality Improvements in Baseline C, XCRY-GSEG-EOPG-TN-15-00004 Issue 3, ESRIN, Italy.

Bouffard, J., Féménias, P., Parrinello, T., 2016. CryoSat mission: data quality status and next product evolutions. Paper presented at the European Space Agency Living Planet Symposium, Prague, May 9–13.

Calafat, F.M., Cipollini, P., Bouffard, J., Snaith, H., Féménias, P., 2017. Evaluation of new CryoSat-2 products over the ocean. Rem. Sens. Environ. 191, 131–144. http://dx.doi.org/10.1016/j.rse.2017.01.009.

Carrère, L., Lyard, F., 2003. Modeling the barotropic response of the global ocean to atmospheric wind and pressure forcing – comparisons with observations. Geophys. Res. Lett. 30 (6), 1275. http://dx.doi.org/10.1029/2002GL016473.

Chelton, D.B., Walsh, E.J., MacArthur, J.L., 1989. Pulse compression and sea level tracking in satellite altimetry. J. Atmos. Ocean. Technol. 6, 407–438. http://dx.doi.org/10.1175/1520-0426(1989)006<0407:PCASLT>2.0.CO;2.

Chelton, D.B., deSzoeke, R.A., Schlax, M.G., Naggar, K.E., Siwertz, N., 1998. Geographical variability of the first Baroclinic Rossby radius of deformation. J. Phys. Oceanogr. 28, 433–460. http://dx.doi.org/10.1175/1520-0485(1998)028<0433:GVOTFB>2.0.CO;2.

Chelton, D.B., Ries, J.C., Haines, B.J., Fu, L.-L., Callahan, P.S., 2001. Satellite altimetry. In: Fu, L.-L., Cazenave, A. (Eds.), Satellite Altimetry and Earth Sciences: A Handbook of Techniques and Applications, Int. Geophys., vol. 69. Academic Press, San Diego, California, pp. 1–131. http://dx.doi.org/10.1016/S0074-614(01)80146-7.

Dee, D.P., Uppala, S.M., Simmons, A.J., Berrisford, P., Poli, P., Kobayashi, S., Andrae, U., Balmaseda, M.A., Balsamo, G., Bauer,

P., Bechtold, P., Beljaars, A.C.M., van de Berg, L., Bidlot, J., Bormann, N., Delsol, C., Dragani, R., Fuentes, M., Geer, A.J., Haimberger, L., Healy, S.B., Hersbach, H., Hólm, E.V., Isaksen, L., Kållberg, P., Köhler, M., Matricardi, M., McNally, A.P., Monge-Sanz, B.M., Morcrette, J.-J., Park, B.-K., Peubey, C., de Rosnay, P., Tavolato, C., Thépaut, J.-N., Vitart, F., . The ERA-Interim reanalysis: configuration and performance of the data assimilation system. Quart. J. R. Met. Soc. 137 (656), 553–597. http://dx.doi.org/10.1002/qj.828.

Dufau, C., Martin-Puig, C., Moreno, L., 2011. User requirements in the coastal ocean for satellite altimetry. In: Vignudelli, S. et al. (Eds.), Coastal Altimetry. Springer, Berlin Heidelberg, pp. 51–60. http://dx.doi.org/10.1007/978-3-642-12796-0_3.

European Space Agency, 2016. Geographical Mode Mask. Online at <https://earth.esa.int/web/guest/-/geographical-mode-mask-7107> (as of 27 April 2016).

Fenoglio-Marc, L., Dinardo, S., Scharroo, R., Roland, A., Dutour Sikric, M., Lucas, B., Becker, M., Benveniste, J., Weiss, R., 2015. The German bight: a validation of CryoSat-2 altimeter data in SAR mode. Adv. Space Res. 55 (11), 2641–2656. http://dx.doi.org/10.1016/j.asr.2015.02.014.

Gómez-Enri, J., Vignudelli, S., Quartly, G.D., Gommenginger, C.P., Cipollini, P., Challenor, P.G., Benveniste, J., 2010. Modeling Envisat RA-2 waveforms in the coastal zone: case study of calm water contamination. IEEE Geosci. Rem. Sens. Lett. 7 (3), 474–478. http://dx.doi.org/10.1109/LGRS.2009.2039193.

Gommenginger, C., Thibaut, P., Fenoglio-Marc, L., Quartly, G., Deng, X., Gómez-Enri, J., Challenor, P., Gao, Y., 2011. Retracking altimeter waveforms near the coasts. In: Vignudelli, S. et al. (Eds.), Coastal Altimetry. Springer, Berlin Heidelberg, pp. 61–101. http://dx.doi.org/10.1007/978-3-642-12796-0_4.

Hollander, M., Wolfe, D.A., Chicken, E., 2013. Nonparametric Statistical Methods, third ed. John Wiley & Sons, Inc., Hoboken, New Jersey.

Koch, K.-R., 1999. Parameter Estimation and Hypothesis Testing in Linear Models, Second, updated and enlarged Edition. Springer-Verlag.

Komjathy, A., Born, G.H., 1999. GPS-based ionospheric corrections for single frequency radar altimetry. J. Atmos. Sol.-Terr. Phys. 61 (16), 1197–1203. http://dx.doi.org/10.1016/S1364-6826(99)00051-6.

Lyard, F., Lefevre, F., Letellier, T., Francis, O., 2006. Modelling the global ocean tides: modern insights from FES2004. Ocean Dyn. 120 (12), 394–415. http://dx.doi.org/10.1007/s10236-006-0086-x.

Mercier, F., Dibarboure, G., Dufau, C., Carrere, L., Thibaut, P., Obligis, E., Labroue, S., Ablain, M., Sicard, P., Garcia, G., Moreau, T., Commien, L., Picot, N., Lambin, J., Bronner, E., Lombard, A., Cazenave, A., Bouffard, J., Gennero, M.C., Seyler, F., Kosuth, P., Bercher, N., 2008. Improved Jason-2 altimetry products for coastal zones and continental waters (PISTACH project). Paper presented at the Ocean Surface Topography Science Team Meeting, Nice, November 10–15.

Nielsen, K., Stenseng, L., Andersen, O.B., Villadsen, H., Knudsen, P., 2015. Validation of CryoSat-2 SAR mode based lake levels. Rem. Sens. Environ. 171, 162–170. http://dx.doi.org/10.1016/j.rse.2015.10.023.

Obligis, E., Desportes, C., Eymard, L., Fernandes, M.J., Lázaro, C., Nunes, A.L., 2011. Tropospheric corrections for coastal altimetry. In: Vignudelli, S. et al. (Eds.), Coastal Altimetry. Springer, Berlin Heidelberg, pp. 147–176. http://dx.doi.org/10.1007/978-3-642-12796-0_6.

Ophaug, V., Breili, K., Gerlach, C., 2015. A comparative assessment of coastal mean dynamic topography in Norway by geodetic and ocean approaches. J. Geophys. Res. Oceans 120 (12), 7807–7826. http://dx.doi.org/10.1002/2015JC011145.

Pugh, D., Woodworth, P.L., 2014. Sea-Level Science: Understanding Tides, Surges, Tsunamis and Mean Sea-Level Changes. Cambridge Univ. Press, Cambridge, U.K.

Revhaug, I., 2007. Outlier detection in multiple testing using Students t-test and Fisher F-test. Kart og Plan 67, 101–107.

Roblou, L., Lamouroux, J., Bouffard, J., Lyard, F., Le Hénaff, M., Lombard, A., Marsalaix, P., De Mey, P., Birol, F., 2011. Post-processing altimeter data toward coastal applications and integration into coastal models. In: Vignudelli, S. et al. (Eds.), Coastal Altimetry. Springer, Berlin Heidelberg, pp. 217–246. http://dx.doi.org/10.1007/978-3-642-12796-0_9.

Saraceno, M., Strub, P.T., Kosro, P.M., 2008. Estimates of sea surface height and near-surface alongshore coastal currents from combinations of altimeters and tide gauges. J. Geophys. Res. Oceans 113, C11013. http://dx.doi.org/10.1029/2008JC004756.

Scagliola, M., Fornari, M., 2017. Known biases in CryoSat-2 Level 1b Products. DOC: C2-TN-ARS-GS-5135, 2.1.

Scharroo, R., Leuliette, E.W., Lillibridge, J.L., Byrne, D., Naeije, M.C., Mitchum, G.T., 2013. RADS: consistent multi-mission products. In: Proc. of the Symposium on 20 Years of Progress in Radar Altimetry, ESA SP-710, ESA Publications Division, European Space Agency, Noordwijk, The Netherlands, 4 pp.

Smith, W.H.F., Scharroo, R., 2009. Mesoscale ocean dynamics observed by satellite altimeters in non-repeat orbits. Geophys. Res. Lett. 36, L06601. http://dx.doi.org/10.1029/2008GL036530.

Stenseng, L., Andersen, O.B., 2012. Preliminary gravity recovery from CryoSat-2 data in the Baffin Bay. Adv. Space Res. 50 (8), 1158–1163. http://dx.doi.org/10.1016/j.asr.2012.02.029.

Valladeau, G., Thibaut, P., Picard, B., Poisson, J.C., Tran, N., Picot, N., Guillot, A., 2015. Using SARAL/AltiKa to improve Ka-band altimeter measurements for coastal zones, hydrology and ice: the PEACHI prototype. Mar. Geod. 38, 124–142. http://dx.doi.org/10.1080/01490419.2015.1020176.

Verron, J., Sengenes, P., Lambin, J., Noubel, J., Steunou, N., Guillot, A., Picot, N., Coutin-Faye, S., Sharma, R., Gairola, R.M., Raghava Murthy, D.V.A., Richman, J.G., Griffin, D., Pascual, A., Rémy, F., Gupta, P.K., 2015. The SARAL/AltiKa altimetry satellite mission. Mar. Geod. 38, 2–21. http://dx.doi.org/10.1080/01490419.2014.1000471.

Vignudelli, S., Cipollini, P., Roblou, L., Lyard, F., Gasparini, G.P., Manzella, G., Astraldi, M., 2005. Improved satellite altimetry in coastal systems: case study of the Corsica Channel (Mediterranean Sea). Geophys. Res. Lett. 32, L07608. http://dx.doi.org/10.1029/2005GL022602.

Vignudelli, S., Kostianoy, A.G., Cipollini, P., Benveniste, J. (Eds.), 2011. Coastal Altimetry. Springer, Berlin Heidelberg. http://dx.doi.org/10.1007/978-3-642-12796-0.

Weatherall, P., Marks, K.M., Jakobsson, M., Schmitt, T., Tani, S., Arndt, J.E., Rovere, M., Chayes, D., Ferrini, V., Wigley, R., 2015. A new digital bathymetric model of the world's oceans. Earth Space Sci. 2 (8), 331–345. http://dx.doi.org/10.1002/2015EA000107.

Webb, E., Hall, A., 2016. Geophysical Corrections in Level 2 CryoSat Data Products, IDEAS-VEG-IPF-MEM-1288 Version 5.1, ESRIN, Italy.

Wingham, D.J., Francis, C.R., Baker, S., Bouzinac, C., Brockley, D., Cullen, R., de Chateau-Thierry, P., Laxon, S.W., Mallow, U., Mavrocordatos, C., Phalippou, L., Ratier, G., Rey, L., Rostan, F., Viau, P., Wallis, D.W., 2006. CryoSat: a mission to determine the fluctuations in Earth's land and marine ice fields. Adv. Space Res. 37 (4), 841–871. http://dx.doi.org/10.1016/j.asr.2005.07.027.

Woodworth, P.L., Horsburgh, K.J., 2011. Surge models as providers of improved "inverse barometer corrections" for coastal altimetry users. In: Vignudelli, S. et al. (Eds.), Coastal Altimetry. Springer, Berlin Heidelberg, pp. 177–189. http://dx.doi.org/10.1007/978-3-642-12796-0_7.

Woodworth, P.L., Hughes, C.W., Bingham, R.J., Gruber, T., 2012. Towards worldwide height system unification using ocean information. J. Geod. Sci. 2 (4), 302–318. http://dx.doi.org/10.2478/v10156-012-0004-8.

Wunsch, C., Stammer, D., 1997. Atmospheric loading and the oceanic "inverted barometer" effect. Rev. Geophys. 35 (1), 79–107. http://dx.doi.org/10.1029/96RG03037.

Please cite this article in press as: Idžanović, M., et al. Coastal sea level from CryoSat-2 SARIn altimetry in Norway. Adv. Space Res. (2017), http://dx.doi.org/10.1016/j.asr.2017.07.043